Phys. Status Solidi RRL **11**, No. 3, 1600428 (2017) / **DOI** 10.1002/pssr.201600428

pss +++rapid research letters+++
www.pss-rapid.com

Delayed phase separation in growth of organic semiconductor blends with limited intermixing

Johannes Dieterle[*,1], Katharina Broch[2], Heiko Frank[1], Giuliano Duva[1], Timo Storzer[1], Alexander Hinderhofer[1], Jiří Novák[3], Alexander Gerlach[1], and Frank Schreiber[1]

[1] Institut für Angewandte Physik, Universität Tübingen, Auf der Morgenstelle 10, 72076 Tübingen, Germany
[2] Cavendish Laboratory, University of Cambridge, JJ Thomson Avenue, CB3 0HE Cambridge, UK
[3] Central European Institute of Technology and Department of Condensed Matter Physics, Faculty of Science, Masaryk University, Kamenice 5, 62500 Brno, Czech Republic

Received 10 December 2016, revised 23 January 2016, accepted 30 January 2017
Published online 7 February 2017

Keywords organic semiconductors, picene, pentacene, phase separation, thin films, X-ray diffraction, blends

[*] Corresponding author: e-mail johannes.dieterle@uni-tuebingen.de, Phone: +49-7071-2976333, Fax: +49-7071-295110

Binary mixed thin films of picene ($C_{22}H_{14}$, PIC) and pentacene ($C_{22}H_{14}$, PEN) consist of crystallites with a statistical occupation of the lattice sites by either PEN or PIC and unit cell parameters continuously changing with the mixing ratio. For high PIC ratios a PIC phase forms which corresponds to a limited intermixing of the two compounds. The growth behavior of these mixtures is investigated *in situ* and in real-time using grazing incidence X-ray diffraction. We observe a delayed phase separation in PIC-rich blends, i.e. complete intermixing in the monolayer range and the nucleation of a pure PIC-phase in addition to the intermixed phase starting from the second monolayer.

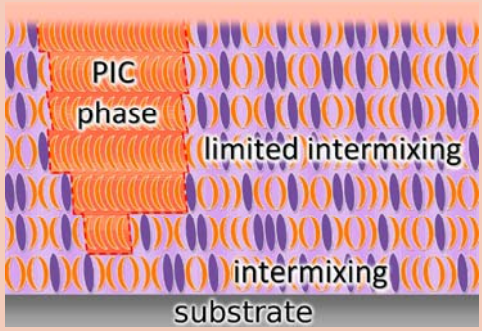

Growth scenario of picene-rich pentacene-picene blends.

1 Introduction Organic semiconductors (OSCs) have evolved to a promising alternative to inorganic materials as functional parts in various organic electronic and optoelectronic applications. Advantages are for example potentially low preparation costs and applicability on flexible substrates [1–5]. For many applications such as organic field effect transistors [6], organic light emitting diodes [7, 8] and solar cells [9, 10] mixtures of OSCs are investigated. The optical and electronic properties important for applications depend on the structural properties such as crystallinity and degree of intermixing and on the morphology [11–16]. The mechanisms of growth and structure formation in OSCs and mixtures of OSCs in thin films are quite complex and not yet well understood [17–20]. Polymorphism and coexistence of polymorphs are rather typical and fundamental issues in molecular crystals, which are notoriously hard to predict and understand theoretically. Therefore, a solid experimental study is even more important [21–28]. For mixed systems, the spectrum of possible scenarios is even broader and its rationalization more challenging. In this context, real-time studies are particularly powerful in helping to assign and understand phases, in particular in the case of phase coexistence, since the temporal evolution can provide clues to the assignment of Bragg reflexions. Also, the kinetics of the phase evolution is a challenge in its own right. Mixing scenarios comprise extreme cases such as continuous statistical intermixing, formation of mixed crystal phases with defined stoichiometry and phase separation [25, 29, 30] depending on sterical properties and chemical composition [31–33]. Recently, a study of the structural properties of the OSC picene [34–36] ($C_{22}H_{14}$, PIC) was reported and showed

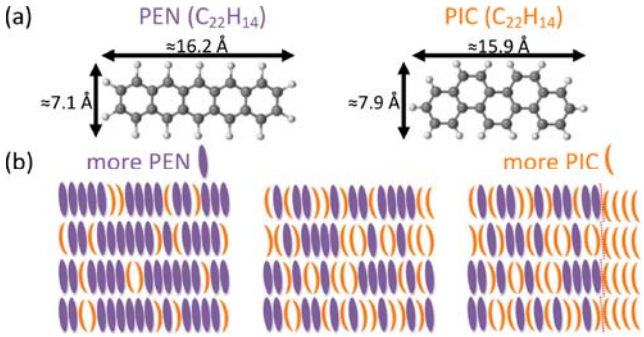

Figure 1 (a) Molecular structure of PEN and PIC. The molecular dimensions are the sum of the atomic distances from the crystal structures [42, 43] and the van der Waals radii. (b) Schematic of the mixing behavior (side view) of PEN : PIC: continuous intermixing and pure PIC excess phase for high PIC concentrations [41].

changes of the in-plane structure with increasing film thickness [37]. For mixtures of PIC and the structurally quite similar isomeric (see Fig. 1a) OSC pentacene [38–40] ($C_{22}H_{14}$, PEN) we reported statistical intermixing with a continuous change of the lattice parameters for PEN rich mixtures and lattice parameters similar to those of PIC for PIC rich mixtures [41]. For high PIC fractions a PIC excess phase forms, indicative of limited intermixing of the two compounds (see Fig. 1b). This result was one of the most surprising findings of our previous study, but can, in a simple picture, be understood by the fact that PIC is slightly shorter than PEN. A common mixed phase requires a sufficiently large lattice spacing for PEN which results in energetically unfavorable large PIC–PIC distances. Hence, as the number of PIC molecules in the film exceeds the number of PEN molecules, an energetically more favorable PIC excess phase is formed with unit cell parameters similar to the pure film phase of PIC. Since structure formation and interface induced effects are important for applications, an understanding of the mechanisms of this limited intermixing and its evolution during film growth would be of high interest. Therefore, we report here a detailed investigation of the growth behavior of PEN : DIP mixtures performed *in situ* and in real-time using grazing incidence X-ray diffraction (GIXD).

2 Experimental Mixed thin films of PIC (purchased from NARD Co. with 99.9% purity) and PEN (purchased from Sigma Aldrich, 99.9% purity) were grown by organic molecular beam deposition [18, 44] on Si substrates covered with a native oxide layer and on fused silica substrates at a substrate temperature of 302 K. The rates were monitored by a quartz crystal micro balance calibrated by X-ray reflectivity. The structural properties of a PIC and a PEN dominated mixture with a growth rate of 1 Å/min were investigated *in situ* and in real time in a portable UHV chamber [45] by GIXD at beamline X04SA [46] of the SLS (Switzerland). The photon energy was 14 keV which corresponds to a wavelength of $\lambda = 0.886$ Å resulting in a critical angle of $\alpha_c = 0.094°$ for PEN and $\alpha_c = 0.128°$ for Si. Directly after growth, XRR scans and GIXD scans with two different angles of incidence ($\alpha_i = 0.04°$ and $\alpha_i = 0.1°$) were performed to obtain depth-resolved structural information.

3 Results and discussion In order to first provide an overview of the resulting structures, Fig. 2 shows post-

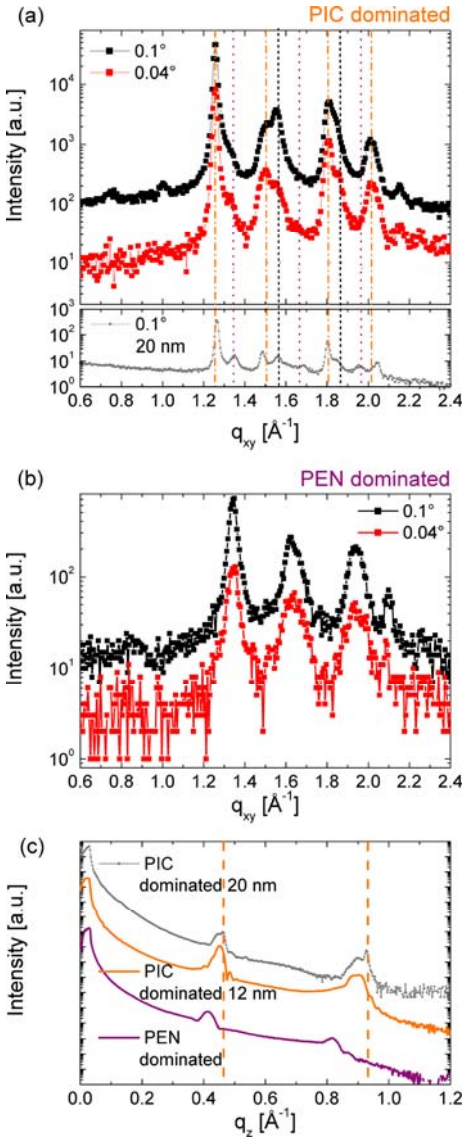

Figure 2 GIXD of PEN : PIC mixtures measured at two different angles of incidence for (a) a PIC dominated (mixing ratio ~1 : 5) and (b) a PEN dominated (mixing ratio 4 : 1) mixture. The orange (black) lines indicate positions of Bragg reflections of PIC L (H) domains. The purple lines correspond to the positions of pure PEN Bragg reflections. For the PIC-dominated mixture (a) the difference in the spectra for different angles of incidence (i.e. penetration depths) indicates that the film structure is not homogeneous throughout the film along the *z*-direction. (c) Corresponding XRR data of the same mixture. The orange lines indicate positions of Bragg reflections of PIC.

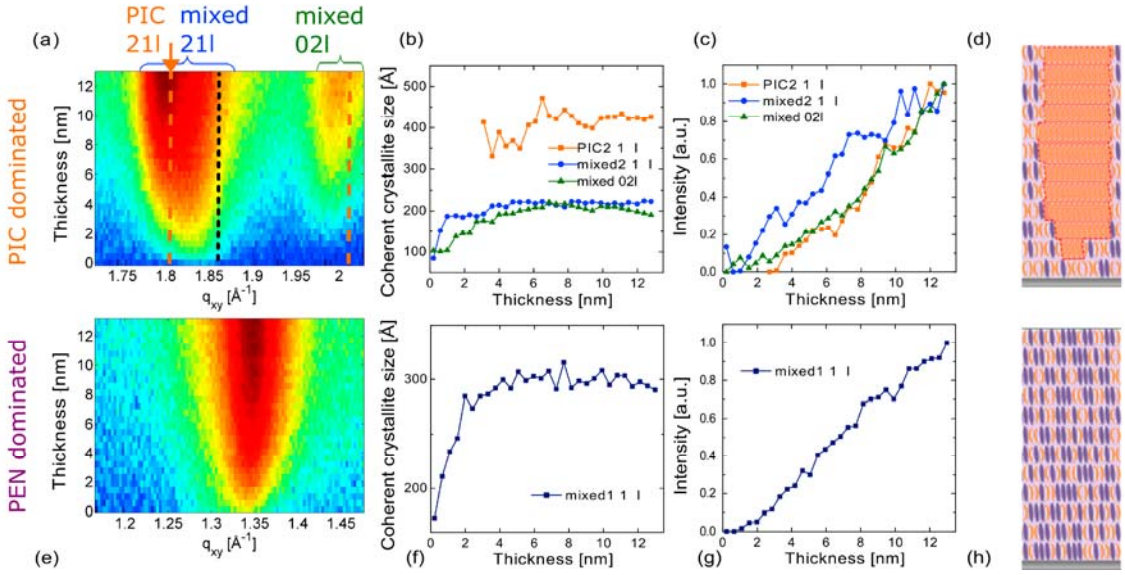

Figure 3 Real-time GIXD (angle of incidence $\alpha_i = 0.1°$) of (a) a PIC- and (e) a PEN-dominated PEN:PIC mixture. The orange (black) lines indicate positions of Bragg reflections of PIC L (H) domains. Extracted coherent scattering island sizes (b) and (f) and normalized intensity evolution (c) and (g). Schematic of the film structure of a PIC-dominated PEN:PIC mixture (d). The mixed film grows crystalline from the beginning. Upon the nucleation of the PIC excess phase the PEN concentration in the mixed phase increases.

growth GIXD scans with different angles of incidence which provide depth-resolved information on mixtures grown at room temperature (302 K) with a growth rate of 1 Å/min. The penetration depth d can be approximated by [47] $d \approx \lambda/(2\pi\sqrt{\alpha_c^2 - \alpha_i^2})$ where α_i is the angle of incidence. This results in $d = 9.5$ nm for $\alpha_i = 0.04°$. For $\alpha_i = 0.1°$, which is above α_c of the film but below α_c of the substrate, the entire film is penetrated. For the PIC-dominated mixture (Fig. 2a) the peaks coincide with those observed for pure PIC corresponding to two different phases H and L [37]. The peaks of the L phase are clearly more pronounced compared to the ones of the H phase for small angles of incidence where the surface of the film contributes more to the signal than for larger angles of incidence. This is comparable to pure PIC where the H domains nucleate prior to the L domains [37]. For the PEN-dominated mixture only peaks of the mixed phase are observed without an apparent difference for the two angles of incidence. In the XRR data (Fig. 2c) for the PIC-dominated mixture the Bragg peaks are split with shoulders at the positions of pure PIC, which can be seen clearly in the data of the thicker PIC-dominated mixture. For the PEN-dominated mixture, however, the Bragg peaks are not split. This indicates the presence of pure PIC domains as well as intermixed domains in the PIC-dominated mixture with a slightly different out-of-plane lattice spacing and an in plane-spacing similar to the H polymorph in pure PIC.

To follow the evolution of this thickness dependence of the structural properties real-time GIXD measurements were performed. For the PIC-dominated mixture the peak with the most pronounced thickness dependence was investigated around $q_{xy} \approx 1.82$ Å^{-1} (Fig. 3a) and for the PEN-dominated the sharpest one around $q_{xy} \approx 1.34$ Å^{-1} (Fig. 3e). For both mixtures Bragg peaks are visible from the first ML (≈1.6 nm). Therefore, it can be concluded that in the beginning a crystalline mixed phase grows. Accordingly for the PEN-dominated mixture the intensity of the investigated peak increases continuously (Fig. 3g) since there is only the intermixed phase. For the PIC-dominated mixture, however, the two phases exhibit different growth dynamics. After one ML the H phase is formed and after the second ML an additional peak occurs at $q_{xy} \approx 1.8$ Å^{-1} which corresponds to the PIC $(\pm 2 \pm 1l)$ reflections of the L phase (Fig. 3a, marked by orange arrow) i.e. the PIC excess phase forms. This peak is overlapping with a much broader peak from the intermixed phase at $q_{xy} \approx 1.82$ Å^{-1}. The extracted coherent scattering island size shown in Fig. 3b and f saturates after ~2 ML for both mixtures. The differences in nucleation behavior are consistent with the depth resolved information obtained from the post growth GIXD scans and are further supported by optical spectroscopy taken during growth which will be published soon.

These observations result in the growth scenario illustrated in Fig. 3d. For small film thicknesses there is complete intermixing. As the film thickness increases a separate PIC-phase is formed to avoid strain. As discussed in Ref. [41] the limited intermixing in the PIC-rich PEN:PIC mixtures is comparable to the mixing behavior reported for thin film mixtures of 6T and p-sexiphenyl (6T:6P) [25]. In a simplified picture this phase separation can be explained by the smaller length of PIC compared to PEN that allows an intercalation of PIC molecules in a PEN rich phase, but causes a too small lattice spacing in a PIC rich phase for intercalation of PEN. In this simplified picture the delayed phase separation reported here can be explained by the fact that the length difference of PEN and PIC is irrelevant in the

first ML. This effect is different from kinetically limited phase separation as observed for example in mixtures of diindenoperylene and buckminsterfullerenes where at the beginning of growth a non crystalline mixed phase forms [30]. The data does not show a continuous increase of the coherent crystallite size as observed in other mixtures with coexisting phases [48]. Blends of PEN with diindenoperylene show a very similar mixing behavior [33] with the important difference that the long-range order parallel to the substrate surface is reduced significantly. The corresponding broadening of the Bragg-peaks makes it difficult to determine if PEN phase-separates in PEN-rich PEN : DIP blends. Therefore, a comparison of PEN : PIC blends with blends of α-sexithiophene (6T) and p-sexiphenyl (6P) [25] is more interesting. In both systems in the blends dominated by the shorter compound (PIC respectively 6T) phase separation occurs. Interestingly in the pure PIC [37] and 6T [27] thin films different polymorphs nucleate, thus this could be another reason for the phase separation.

4 Conclusion We have investigated the influence of the formation of the PIC excess phase which accompanies the statistically mixed PEN : PIC phase on the growth and mixing behavior *in situ* and in real-time as well as depth-resolved after growth. For PIC-rich mixtures we observe a delayed phase separation. Our real-time measurements allow for a detailed investigation of the growth dynamics of the different phases. At the beginning a crystalline mixed phase forms and later additionally a PIC excess phase forms leading to a decrease of the PIC fraction in the mixed phase. The size of coherently scattering islands increases rapidly in the beginning for PEN- and PIC-dominated mixtures and saturates after 2 ML. Post-growth depth-resolved measurements are consistently showing an increased relative intensity of peaks related to the PIC excess phase in the top layers. Since this effect is observed for a low growth rate of 1 Å/min, it is likely not merely a kinetic effect but rather a surface-induced one caused by the difference in the sterical properties.

Acknowledgements We acknowledge the Paul Scherrer Institut, Villigen, Switzerland for provision of synchrotron radiation beamtime at beamline X04SA of the SLS and would like to thank Nicola Casati for technical assistance. The research leading to these results has received funding from the European Community's Seventh Framework Programme (FP7/2007-2013) and from the DAAD. K.B. and F.S. acknowledge support of the Deutsche Forschungsgemeinschaft (BR4869/1-1, SCHR700/24-1). G.D. acknowledges support from the Carl Zeiss Stiftung. J.N. acknowledges support from the project CEITEC 2020 (grant no. LQ1601 financed by the MEYS of the Czech Republic).

References

[1] S. R. Forrest, Nature **428**, 911–918 (2004).
[2] W. Brütting and C. Adachi, Physics of organic semiconductors, 2nd edn. (Wiley-VCH, Weinheim, 2012).
[3] S. Ahmad, J. Polym. Eng. **34**(4), 279–338 (2014).
[4] G. Witte and C. Wöll, Phys. Status Solidi A **205**(3), 497–510 (2008).
[5] J. Lewis, Mater. Today **9**(4), 38–45 (2006).
[6] H. Sirringhaus, Adv. Mater. **26**(9), 1319–1335 (2014).
[7] J. H. Jou, S. Kumar, A. Agrawal, T. H. Li, and S. Sahoo, J. Mater. Chem. C **3**(13), 2974–3002 (2015).
[8] N. Thejo Kalyani and S. Dhoble, Renew. Sustain. Energy Rev. **16**(5), 2696–2723 (2012).
[9] W. Cao and J. Xue, Energy Environ. Sci. **7**(7), 2123 (2014).
[10] J. Yu, Y. Zheng, and J. Huang, Polymers **6**(9), 2473–2509 (2014).
[11] R. Hesse, W. Hofberger, and H. Bässler, Chem. Phys. **49**, 201 (1980).
[12] K. O. Lee and T. T. Gan, Chem. Phys. Lett. **51**, 120–124 (1977).
[13] Y. Yoshida, H. Takiguchi, T. Hanada, N. Tanigaki, E. M. Han, and K. Yase, J. Cryst. Growth **198–199**(2), 923–928 (1999).
[14] K. Kolata, T. Breuer, G. Witte, and S. Chatterjee, ACS Nano **8**(7), 7377–7383 (2014).
[15] A. Opitz, J. Wagner, W. Brütting, A. Hinderhofer, and F. Schreiber, Phys. Status Solidi A **206**(12), 2683–2694 (2009).
[16] S. Heutz, P. Sullivan, B. Sanderson, S. Schultes, and T. Jones, Sol. Energy Mater. Sol. Cells **83**, 229–245 (2004).
[17] A. C. Dürr, F. Schreiber, K. A. Ritley, V. Kruppa, J. Krug, H. Dosch, and B. Struth, Phys. Rev. Lett. **90**(1), 016104 (2003).
[18] F. Schreiber, Phys. Status Solidi A **201**(6), 1037–1054 (2004).
[19] S. Kowarik, K. Broch, A. Hinderhofer, A. Schwartzberg, J. O. Ossó, D. Kilcoyne, F. Schreiber, and S. R. Leone, J. Phys. Chem. C **114**, 13061 (2010).
[20] S. Kowarik, A. Gerlach, A. Hinderhofer, S. Milita, F. Borgatti, F. Zontone, T. Suzuki, F. Biscarini, and F. Schreiber, Phys. Status Solidi RRL **2**(3), 120–122 (2008).
[21] B. Wedl, R. Resel, G. Leising, B. Kunert, I. Salzmann, M. Oehzelt, N. Koch, A. Vollmer, S. Duhm, O. Werzer, G. Gbabode, M. Sferrazza, and Y. Geerts, RSC Adv. **2**(10), 4404–4414 (2012).
[22] I. Salzmann, S. Duhm, G. Heimel, J. P. Rabe, N. Koch, M. Oehzelt, Y. Sakamoto, and T. Suzuki, Langmuir **24**(14), 7294–7298 (2008).
[23] J. Bernstein, Polymorphism in molecular crystals (International Union of Crystallography, 2002).
[24] J. Bernstein, J. Phys. D: Appl. Phys. **26**, B66–B76 (1993).
[25] J. O. Vogel, I. Salzmann, S. Duhm, M. Oehzelt, J. P. Rabe, and N. Koch, J. Mater. Chem. **20**(20), 4055–4066 (2010).
[26] A. O. F. Jones, B. Chattopadhyay, Y. H. Geerts, and R. Resel, Adv. Funct. Mater. **26**(14), 2233–2255 (2016).
[27] C. Lorch, R. Banerjee, C. Frank, J. Dieterle, A. Hinderhofer, A. Gerlach, and F. Schreiber, J. Phys. Chem. C **119**(1), 819–825 (2015).
[28] H. Méndez, G. Heimel, S. Winkler, J. Frisch, A. Opitz, K. Sauer, B. Wegner, M. Oehzelt, C. Röthel, S. Duhm, D. Többens, N. Koch, and I. Salzmann, Nature Commun. **6**(10), 8560 (2015).
[29] J. P. Reinhardt, A. Hinderhofer, K. Broch, U. Heinemeyer, S. Kowarik, A. Vorobiev, A. Gerlach, and F. Schreiber, J. Phys. Chem. C **116**(20), 10917–10923 (2012).

[30] R. Banerjee, J. Novák, C. Frank, C. Lorch, A. Hinderhofer, A. Gerlach, and F. Schreiber, Phys. Rev. Lett. **110**(18), 185506 (1–5) (2013).
[31] A. Kitaigorodsky, Mixed Crystals (Springer, Berlin, Heidelberg, 1984).
[32] A. Hinderhofer and F. Schreiber, Chem. Phys. Chem. **13**(3), 628–643 (2012).
[33] A. Aufderheide, K. Broch, J. Novák, A. Hinderhofer, R. Nervo, A. Gerlach, R. Banerjee, and F. Schreiber, Phys. Rev. Lett. **109**, 156102 (2012).
[34] A. De, R. Ghosh, S. Roychowdhury, and P. Roychowdhury, Acta Crystallogr. **41**(6), 907–909 (1985).
[35] R. Mitsuhashi, Y. Suzuki, Y. Yamanari, H. Mitamura, T. Kambe, N. Ikeda, H. Okamoto, A. Fujiwara, M. Yamaji, N. Kawasaki, Y. Maniwa, and Y. Kubozono, Nature **464**(7285), 76–79 (2010).
[36] N. Kawasaki, Y. Kubozono, H. Okamoto, A. Fujiwara, and M. Yamaji, Appl. Phys. Lett. **94**(4), 043310 (2009).
[37] T. Hosokai, A. Hinderhofer, F. Bussolotti, K. Yonezawa, C. Lorch, A. Vorobiev, Y. Hasegawa, Y. Yamada, Y. Kubozoro, A. Gerlach, S. Kera, F. Schreiber, and N. Ueno, J. Phys. Chem. C **119**(52), 29027–29037 (2015).
[38] N. Koch, Chem. Phys. Chem. **8**(10), 1438–1455 (2007).
[39] G. Wang, Y. Luo, and P. H. Beton, Appl. Phys. Lett. **83**(15), 3108–3110 (2003).
[40] A. Troisi, Chem. Soc. Rev. **40**(5), 2347 (2011).
[41] J. Dieterle, K. Broch, A. Hinderhofer, H. Frank, J. Novák, A. Gerlach, T. Breuer, R. Banerjee, G. Witte, and F. Schreiber, J. Phys. Chem. C **119**(47), 26339–26347 (2015).
[42] R. B. Campbell, J. M. Robertson, and J. Trotter, Acta Crystallogr. **14**, 705–711 (1961).
[43] A. De, R. Ghosh, S. Roychowdhury, and P. Roychowdhury, Acta Crystallogr. **41**(6), 907–909 (1985).
[44] G. Witte and C. Wöll, J. Mater. Res. **19**(7), 1889–1916 (2004).
[45] K. A. Ritley, B. Krause, F. Schreiber, and H. Dosch, Rev. Sci. Instrum. **72**, 1453–1457 (2001).
[46] P. R. Willmott, D. Meister, S. J. Leake, M. Lange, A. Bergamaschi, M. Böge, M. Calvi, C. Cancellieri, N. Casati, A. Cervellino, Q. Chen, C. David, U. Flechsig, F. Gozzo, B. Henrich, S. Jäggi-Spielmann, B. Jakob, I. Kalichava, P. Karvinen, J. Krempasky, A. Lüdeke, R. Lüscher, S. Maag, C. Quitmann, M. L. Reinle-Schmitt, T. Schmidt, B. Schmitt, A. Streun, I. Vartiainen, M. Vitins, X. Wang, and R. Wullschleger, J. Synchrotron Radiat. **20**(5), 667–682 (2013).
[47] M. Tolan, X-ray scattering from soft-matter thin films: Materials science and basic research, Springer tracts in modern physics (Springer, Berlin, London, 1999).
[48] K. Broch, A. Gerlach, C. Lorch, J. Dieterle, J. Novák, A. Hinderhofer, and F. Schreiber, J. Chem. Phys. **139**(17), 174709 (2013).